Advances in Environmental Research, *Vol. 6, No. 2 (2017) 95-111*
DOI: https://doi.org/10.12989/aer.2017.6.2.095

Valorization of swine manure into low cost activated carbons capable of Cr(VI) removal

Lenia Gonsalvesh[1], Grazyna Gryglewicz[2], Robert Carleer[3] and Jan Yperman*[3]

[1]Institute of Organic Chemistry, Bulgarian Academy of Sciences, Sofia 1113, Bulgaria
[2]Department of Polymer and Carbonaceous Materials, Faculty of Chemistry,
Wrocław University of Technology, 50-344 Wrocław, Poland
[3]Research group of Applied and Analytical Chemistry, Hasselt University, B-3590 Diepenbeek, Belgium

(Received September 9, 2016, Revised May 15, 2017, Accepted May 16, 2017)

Abstract. The valorization of swine manure samples, i.e., de-watered cake (SMc) and solid digestate (SMd), in products with beneficial value, i.e., low cost activated carbons (ACs), is studied. For this purpose slow pyrolysis and steam activation at three different duration times are applied. Additionally, the obtained ACs are characterized and tested towards removal of Cr(VI) from aqueous solutions. It is revealed that BET surface area varies in the range of 236-267 m^2/g for ACs prepared from SMc sample and in the range of 411-432 m^2/g for ACs prepared from SMd sample. Despite the low determined surface area of prepared ACs, a high total Cr removal capacity is observed occurring through a "coupled adsorption-reduction" mechanism. Higher Cr(VI) removal capacity is demonstrated for ACs having higher surface area (q_m is 140.9 mg/g according Langmuir modelling). Cr(VI) removal is found to be pH dependent with a maximum at pH 1. However at that pH significant amounts of Cr remain in the solution as Cr(III). At pH 2 lower amount of Cr(VI) is removed compensated by a higher removal of Cr(III) resulting in a higher amount of adsorbed Cr_{tot}. Therefore adsorption at pH 2 is found to be appropriate. The removal capacity of the studied ACs towards Cr(VI) is almost independent of activation time.

Keywords: manure; activated carbon; chromium; adsorption

1. Introduction

The increased worldwide manure concentrations and increased environmental requirements and regulations towards emissions originating from it (NH_3, NO_x, methane and non-methane volatile organic compounds and particulate matter) (European Environment Agency 2009) have evoked an amplified interest towards its management. Currently, a number of pathways, i.e., anaerobic and aerobic digestions, composting, flocculation, etc., have been developed in order to valorize swine manure (SM) and to limit its negative environmental impact with respect to surface water, groundwater and air quality, as the lasts are being affected by odors, toxic effluents and gaseous emissions from swine production industries. Nevertheless those technologies suffer from several drawbacks and in some cases contribute to environmental pollution. An alternative option for SM

---

*Corresponding author, Professor, E-mail: jan.yperman@uhasselt.be

http://www.techno-press.org/?journal=aer&subpage=7 ISSN: 2234-1722 (Print), 2234-1730 (Online)

management can be thermochemical conversion, namely pyrolysis, which is not highly explored although it is promising due to the following reasons (Ro *et al.* 2010): i) SM is an abundant biomass source with the potential to be converted into valuable products; ii) the increased volumes of manures impede the use of traditional land application methods for manure management; iii) the advantages of thermochemical conversion of de-watered manure (shorter time of conversion, pathogens destruction, absence of non-biodegradable and toxic sludge and supernatant requiring further treatments and disposal) over biochemical technologies. However the research, elaboration and literature on thermochemical conversion technologies of manures is scarce. The numbers of pyrolysis studies are mostly focused on bio-oil and biochar production from poultry and swine (Schnitzer *et al.* 2008, Xiu *et al.* 2010, Cantrell *et al.* 2012, Ro *et al.* 2010) manures. The produced biochar is mainly used for soil amendments (Uchimiya *et al.* 2012, Cantrell *et al.* 2012). However, alternative manure biochar utilization can be the manufacture of effective adsorbents having broad and important industrial applications, i.e., low cost ACs, capable of removing pollutants from aqueous solutions (Lima and Marshall 2005). Considering the swine manure re-use, this advantageous approach is rather not explored. The utilization of manures for AC preparation is additionally attractive since reduced waste volume for disposal is achieved, respectively costs for waste disposal and pollution are decreased.

ACs are well known adsorbents that depending on their textural properties and surface chemistry are capable of removing different contaminants. In general, the as-received ACs composed mainly of amorphous carbon are rather nonpolar and hydrophobic and thus more suitable for the adsorption of neutral or nonpolar organic compounds. Nevertheless, often the ACs are associated with a certain amount of ash and surface functional groups originating either from the raw precursor and becoming a part of the chemical structure during carbonization/activation, or are associated with additional treatments, i.e., oxidation, nitrification, sulfonation, etc. Thus created acidic and basic surface groups make the carbon surface hydrophilic and enhance the properties of the carbons towards removal of polar and ionic pollutants as heavy metals in waters released from metallurgical and chemical industries.

The main objective of the current research topic is to use pyrolysis as an ecologically sustainable and economically feasible method for SM utilization in products with added value, in particular low cost ACs. Objects of valorisation will be de-watered SM cake and solid digestate, both obtained from a private company. Additionally, the physical and chemical properties as well as adsorption capacity of prepared ACs towards toxic and carcinogenic inorganic pollutants, i.e., chromium (Cr) in aqueous solutions will be studied. The two oxidation states of Cr present in the environment are Cr (III) and Cr (VI). Trivalent chromium is less toxic than the hexavalent form, which is recognized as carcinogenic and mutagenic agent. However, due to the possible oxidation of Cr(III) to Cr(VI), environmental legislation limits both, i.e., total and hexavalent chromium concentration in water (Di Natale *et al.* 2007).

2. Materials and methods

2.1 Materials and sample preparation

Two SM samples are studied, i.e., de-watered SM cake (SMc) and solid digestate (SMd). Prior to use, the samples are grounded, sieved (<2 mm) and oven dried at 110℃. The proximate (i.e., moisture (W), volatile matter (VM), fixed carbon (C_{fix}) and ash content) and ultimate (C, H, N, S

Table 1 Proximate and ultimate analyses of SM samples

Analysis	Samples	
	SMc	SMd
Proximate (wt.%)		
W^{ad}	13.5	8.1
Ash^{db}	21.6	13.8
VM^{db}	56.6	56.8
C_{fix}^{db}	21.8	24.0
Elem. Analysis $(wt.\%)^{db}$		
C	38.6	37.2
H	4.7	4.2
N	2.9	2.0
S	0.8	0.6
O^{diff}	31.4	42.1
Atomic ratios		
H/C	1.45	1.35
N/C	0.07	0.05
S/C	0.01	0.01
O/C	0.61	0.85
HHV* (MJ/kg)	15.3	13.3

^{db} dry basis; ^{ad} air dried; O^{diff}=100-(C+H+N+S+Ash), db; *HHV–higher heating value is calculated on dry basis by the formula of Channiwala

and O content) analyses of both samples as well as Higher Heating Values (HHV) calculated by the formula of Channiwala (Channiwala and Parikh 2002) are presented in Table 1.

2.2 Pyrolysis set-up

Samples are pyrolyzed in oxygen free atmosphere in a previously described lab-scale pyrolysis reactor (Gonsalvesh *et al.* 2016b). Before each experiment the reactor is filled with about 70 g sample and slow heating rate of 10℃/min is applied until the desired pyrolysis temperature is reached. In literature, temperatures within 350-800℃ range are used for production of chars from manure samples (Ro *et al.* 2010, Cantrell *et al.* 2012, Tsai *et al.* 2012, Lima and Marshall 2005). However, in our study a temperature of 500℃ (kept isothermal for 1 h) is chosen for pyrolysis based on TGA analysis of the SM samples. The obtained chars from SMc and SMd samples are respectively marked as c-SMc and c-SMd.

2.3 Physical activation with steam

For steam activation the precursor materials (~8 g), i.e., slow pyrolysis c-SMc and c-SMd chars, are introduced into the quartz tube and the position of the samples is fixed by quartz wool plugs. The tube is inserted in a horizontal furnace, flushed with 60 ml/min N_2 and a temperature program of 35℃/min is applied up to temperature of 800℃. At 800℃ the temperature is held isothermal and the N_2 gas inlet is switched to steam. Three activation duration times are tested, i.e., 30, 45 and 60 min, at a constant steam flow of 330 μL/min provided by a Schott TR 100 automatic burette. Activated carbons obtained through activation for 30, 45 and 60 min from c-SMc char are marked as AC_{30}-SMc, AC_{45}-SMc and AC_{60}-SMc, respectively. Activated carbons received through activation for 30, 45 and 60 min from c-SMd char are marked as AC_{30}-SMd, AC_{45}-SMd and AC_{60}-SMd.

2.4 Characterization of the biomass, chars and activated carbons

The samples are subjected to proximate and ultimate analyses using a DuPont Instrument 951 thermogravimetrical analyser and Thermo Electron Flash EA1113 elemental analyzer, respectively, and to pH_{pzc} determination as described in Stals et al. and Gonsalvesh *et al.* (Stals *et al.* 2010, Gonsalvesh *et al.* 2016b, Gonsalvesh *et al.* 2016a). Textural characterization is carried out by measuring the N_2 adsorption isotherms at -196℃ in an automatic apparatus ASAP2020 sorption analyzer (Micrometrics). Prior to the adsorption measurements the samples are outgassed for 12 h at 250℃. The isotherms are used to calculate specific surface area S_{BET} using BET method (Brunauer *et al.* 1938) and the total pore volume from the total amount of N_2 adsorbed at a relative pressure of $p/p_0=0.98$. The micropore volume (V_{DR}) was determined by applying the Dubinin-Radushkevich method (Stoeckli *et al.* 1999).

2.5 Chromium(VI) adsorption

The initial Cr(VI) solutions are prepared by dissolving $K_2Cr_2O_7$ (oven dried at 105℃ for 1 h) in *Milli-Q* water. The pH of initial solutions is adjusted by adding 0.1 N HCl or 0.1 N NaOH and is not further altered during the adsorption experiments. The batch adsorption experiments are performed in a thermal shaker at a temperature of 25℃ for 24 h using 100 ml Erlenmeyer flasks containing 0.030 g of investigated ACs and 50 ml of Cr(VI) solutions with concentration varying in the range of 10 to 200 mg/L. The exact Cr(VI) concentrations of initial and equilibrium solutions are determined spectrophotometrically after complexing Cr(VI) with 1,5-diphenylcarbohydrazide according to the standard method ASTM D1687-92, Test Method A. The absorbance is measured by Ultrospec 2000 UV-VIS spectrophotometer at wavelength of 540 nm. Total chromium concentrations (Cr_{tot}) in solutions are determined by Perkin Elmer Optima 3000 DV ICP AES device. The concentration of trivalent chromium, Cr(III), in solutions is calculated as the difference between Cr_{tot} and Cr(VI) concentrations. The Cr adsorption capacities are calculated using the equation

$$q_{\mathrm{e}} = \frac{\left(C_0 - C_{\mathrm{e}}\right)V}{m} \tag{1}$$

where q_e is the adsorption capacity at equilibrium (mg/g), C_0 and C_e are the Cr initial and equilibrium concentrations (mg/L), respectively, V is the volume of Cr solutions (L) and m is the weight of AC (g). Adsorption isotherms are obtained by plotting adsorption capacities with respect to equilibrium concentrations. Standardized Langmuir and Freundlich isotherm modelling, described in depth in (Gonsalvesh *et al.* 2016b, Gonsalvesh *et al.* 2016a), is applied to the obtained adsorption data. Nonlinear Langmuir equations can be found in Table 2. K_L (L/mg) and q_m (mg/g) are the Langmuir constants.

Table 2 Adsorption isotherm models

Isotherm	Nonlinear form	Linear form	Plot
Langmuir	$q_\mathrm{e} = \frac{q_\mathrm{m} K_\mathrm{L} C_\mathrm{e}}{1 + K_\mathrm{L} C_\mathrm{e}}$	Langmuir-A, $\frac{C_\mathrm{e}}{q_\mathrm{e}} = \frac{C_\mathrm{e}}{q_\mathrm{m}} + \frac{1}{K_\mathrm{L} q_\mathrm{m}}$ Langmuir-B, $\frac{1}{q_\mathrm{e}} = \frac{1}{K_\mathrm{L} q_\mathrm{m} C_\mathrm{e}} + \frac{1}{q_\mathrm{m}}$	$\frac{C_\mathrm{e}}{q_\mathrm{e}}$ vs C_e $\frac{1}{q_\mathrm{e}}$ vs $\frac{1}{C_\mathrm{e}}$
Freundlich	$q_\mathrm{e} = K_\mathrm{F} C_\mathrm{e}^{1/n}$	$\log q_\mathrm{e} = \frac{1}{n} \log C_\mathrm{e} + \log K_\mathrm{F}$	$\log q_\mathrm{e}$ vs $\log C_\mathrm{e}$

K_L is the sorption equilibrium constant for distribution of adsorbate, while q_m is the maximum adsorption capacity which represents the mass of adsorbate adsorbed in a complete monolayer having one molecule thickness per mass of adsorbent. Values of K_L and q_m can be graphically determined from the linear form of the Langmuir model. Four different linearization types and simple linear regression will result in different Langmuir constants values depending on which of the linearized forms is fitted (Foo and Hameed 2010, Ho 2006). This is because each of these transformations changes the original error distribution (Kinniburgh 1986). The linearization types of Langmuir equation (isotherm models) used in the current study are shown in Table 2 (equations marked as Langmuir-A and Langmuir-B). In general, it is observed that the best fit is obtained using Langmuir-A equation because of the minimal deviations from the fitted equation resulting in the best error distribution (Ho 2006). However, Kinniburgh underlines that the best transformation is not necessarily the one which gives the highest correlation coefficient but rather the one in which the resulting error distribution most closely matches the “true” error distribution (Kinniburgh 1986). The preferred transformation may therefore vary from data set to data set.

An important Langmuir isotherm characteristic can be expressed in terms of a dimensionless separation factor, R_L, defined in the literature (Barkat *et al.* 2009, Khezami and Capart 2005, Duranoğlu *et al.* 2012, Foo and Hameed 2010) as

$$R_\mathrm{L} = \frac{1}{1 + K_\mathrm{L} C_0} \tag{2}$$

The R_L values determine feasibility and favorability of adsorption processes.

The Freundlich model is also a widely used empirical equation which is strictly a curve-fitting model and works very well for many industrial wastewater applications. It is expressed by the equation shown in Table 2, where K_F and n are indicators of adsorption capacity and adsorption intensity, respectively. These constants can be obtained from the intercept and the slope of the linear plot of Freundlich model as shown in Table 2. The slope, ranging between 0 and 1, is a measure for adsorption intensity or surface heterogeneity, becoming more heterogeneous as its value gets closer to zero (Foo and Hameed 2010). A value below unity represents chemisorption processes where 1/n>1is indicative for cooperative adsorption.

Table 3 Pyrolysis products mass balance and characteristics of bio-chars

	Precursors		SMc	SMd
Bio-Char	Code name		c-SMc	c-SMd
	Yields (wt.%)		35.6	37.2
	Proximate (wt.%)	W^{ad}	2.2	2.2
		Ash^{db}	51.4	39.5
		VM^{db}	1.7	6.0
		C_{fix}^{db}	45.9	54.6
	Ultimate (wt.%)^{db}	C	38.6	50.3
		H	1.2	1.1
		N	2.0	1.4
		S	0.4	0.7
		O^{diff}	6.4	7.0
	Atomic ratios	*H/C*	0.36	0.26
		N/C	0.04	0.02
		S/C	0.00	0.00
		O/C	0.12	0.11
	HHV (MJ/kg)*		13.1	17.4
Bio-Oil	Yields (wt.%)		40.4	33.3
Bio-Gas**	Yields (wt.%)		24.0	29.5

O^{diff}=100-(C+H+N+S+Ash), db; *HHV - higher heating value is calculated on dry basis by the formula of Channiwala;** - calculated by difference.

3. Results and discussion

3.1 Bulk characteristics of initial precursors and obtained bio-chars

Based on proximate analyses of initial SMc and SMd precursors, presented in Table 1, it can be seen that both samples are characterized by high ash content, i.e., 21.6 wt.% and 13.8 wt.% for SMc and SMd samples, respectively. The ash content is significantly higher compared to those in crop, wood and some straw (wheat and barley straw) residues but close to that of rice straw (McKendry 2002a, Tsai *et al.* 2012) and comparable to other swine manure wastes (Tsai *et al.* 2012, Cantrell *et al.* 2012, Azuara *et al.* 2013). Considering the volatile matter and fixed carbon contents of raw manure samples, a dominant presence of the volatile matter is revealed. Volatile matter is almost equal for both precursors while the content of fixed carbon is somewhat higher in the case of SMd sample. However, it should be mentioned that the sum of both contents, i.e., the content of volatile matter and fixed carbon or the so called combustible content, is high enough to state that investigated biomasses are rich in organic matter content.

With regard to ultimate analyses of investigated manure biomasses, a relatively high concentration of carbon and oxygen is found. The carbon content is almost identical for both samples. These data are reasonably comparable to other studies on swine manures (Xiu *et al.* 2010, Azuara *et al.* 2013) but lower compared to biomass of vegetable origin (McKendry 2002a, Stals *et al.* 2010, Smets *et al.* 2011). Oxygen content is higher for the digested sample SMd. It should be mentioned as well that the nitrogen and sulphur contents of studied samples are relatively higher compared to forestry and crop residues. According to Tsai *et al*. (2012) this may be attributed to high protein content present in the manures, which are dependent on the dietary feeds, swine species and breeding regions.

The calculated pyrolysis product mass balance (Table 3) revealed that the pyrolysis of SMc sample gives 35.6 wt.% bio-char, 40.4 wt.% bio-oil and 24.0 wt.% bio-gas yields, while during pyrolysis of SMd sample 37.2 wt.% bio-char, 33.3 wt.% bio-oil and 29.5 wt.% bio-gas yields are obtained. Based on McKendry it can be stated that high bio-char yields are achieved in both cases (McKendry 2002b). According to the same author, maximum up to 35% bio-chars yields can be achieved during carbonization or so called slow pyrolysis. The ultimate and proximate analyses of chars as well as HHV are also presented in Table 3. Not surprisingly, the content of C_{fix} of bio-char samples is enhanced compared to the precursors, as the highest amount is found for c-SMd. It can be also seen that both samples are characterized by very high ash content, respectively 51.4% for c-SMc and 39.5% for c-SMd. This ash content is increased for both samples compared to their counterpart precursor mainly due to volatilization during carbonization. With respect to ultimate analysis, higher carbon content is also registered for c-SMd. This is in accordance with C_{fix} and VM contents. It is noteworthy that the oxygen content is significantly reduced compared to that of the precursor samples. This is an indication that oxygen containing polar compounds are rather transferred in bio-oil and/or bio-gas fractions during the carbonization of the precursors than entrapped and rearranged in the bio-char fraction. The decreased O/C and H/C molar ratios for both char samples in comparison with their precursor counterparts are an indication for the removal of oxygen containing compounds as the result of decarboxylation (CO_2 release) and elimination reactions (H_2O).

Table 4 Characteristics of activated carbons

Analysis	Samples					
	AC_{30}-SMc	AC_{45}-SMc	AC_{60}-SMc	AC_{30}-SMd	AC_{45}-SMd	AC_{60}-SMd
Yield (wt. %)	68.9	69.9	64.0	70.0	61.9	57.1
Proximate (wt.%)						
W^{ad}	0.9	1.5	2.1	2.0	1.6	1.2
Ash^{db}	63.8	65.3	71.0	51.5	65.6	67.7
VM^{db}	8.7	2.1	2.2	2.0	3.4	14.5
C_{fix}^{db}	27.5	32.5	25.8	46.5	30.9	17.8
Elem. Analysis $(wt.\%)^{db}$						
C	31.0	33.2	27.8	39.6	33.3	31.1
H	0.4	0.5	0.4	1.0	0.7	0.5
N	0.8	0.8	0.6	0.3	0.2	0.2
S	<DL	<DL	<DL	<DL	<DL	<DL
O^{diff}	4.0	0.3	0.2	7.6	0.2	0.5
Atomic ratios						
H/C	0.17	0.17	0.18	0.29	0.24	0.19
N/C	0.02	0.02	0.02	0.01	0.01	0.01
O/C	0.10	0.01	0.01	0.14	0.00	0.01

DL-detection limit

Table 5 Porous texture parameters determined by N_2 sorption at 77K

Sample	S_{BET}	V_t	V_{mic}	V_{mez}
	m^2/g	cm^3/g	cm^3/g	cm^3/g
AC_{30}-SMc	267	0.222	0.106	0.116
AC_{45}-SMc	236	0.152	0.09	0.062
AC_{60}-SMc	246	0.176	0.094	0.082
AC_{30}-SMd	428	0.190	0.156	0.034
AC_{45}-SMd	432	0.199	0.160	0.039
AC_{60}-SMd	411	0.196	0.151	0.045

3.2 Activated carbons

Characteristics of obtained AC are gathered in Tables 4-5.

The ACs yields, calculated from the weight of resultant ACs divided by the weight of their counterpart bio-char sample, range from 64.0% to 69.9% for ACs prepared from c-SMc, i.e., AC_{30}-SMc, AC_{45}-SMc and AC_{60}-SMc samples, and from 57.1% to 70.0% for ACs prepared from c-SMd, i.e., AC_{30}-SMd, AC_{45}-SMd and AC_{60}-SMd samples. It is revealed that the yields of ACs decrease with increasing activation time in case of AC-SMd samples while it is almost independent for the AC-SMc samples. Comparing the proximate and ultimate analyses of the ACs with those of their corresponding bio-chars, it becomes obvious that increase of the ash content occurs as a result of the activation process at 800℃ due to an additional net carbon loss. Since the ash contents of produced ACs is quite high it is more reasonable to use the term “mineral-carbon sorbent” for description of those products. Nevertheless for simplicity of presentation the ACs terminology is preferred. The increase in ash content and the decrease in C and C_{fix} contents are proportional to the increase of the activation time in case of AC-SMd samples, but less significant in case of the AC-SMc samples. It is not clear at the moment why the AC_{45}-SMc sample behaves a little bit differently.

Inasmuch as oxygen functional groups can influence heavy metals adsorption, it is appropriate to comment ACs oxygen content as well. In general it is observed that the oxygen content of studied ACs as well as of their corresponding bio-chars is low. Nevertheless it is found that the oxygen content is reduced for AC_{30}-SMc sample in comparison with c-SMc, but is rather unchanged for AC_{30}-SMd sample in comparison with c-SMd. By increasing the activation time to 45 min and 60 min, the organic oxygen content is reduced to approximately zero for ACs prepared from both c-SMc and c-SMd.

Textural parameters of ACs can be deduced from N_2 adsorption-desorption isotherms shown in Fig. 1.

It is observed that the isotherms of all studied ACs represent a type I-IV hybrid shape, according to IUPAC classification (Bandosz 2006). The initial parts of the isotherms (at low relative pressure) are very steep (typical for type I isotherms) and reflect the significant role of microporous structure. Inasmuch as at high relative pressure a hysteresis is observed, the isotherms resemble IV shape as well. The appearance of H4 type hysteresis loops in N_2 adsorption-desorption isotherms can be attributed to the presence of mesopores and capillary condensation/evaporation phenomena. From N_2 adsorption-desorption isotherms it can also be revealed that c-SMd based ACs demonstrate higher N_2 adsorption capacity than c-SMc based ACs.

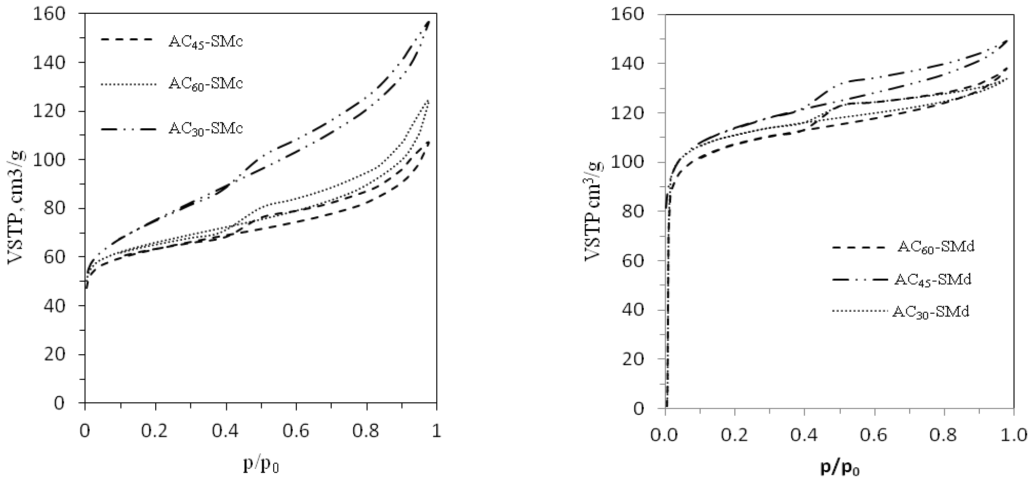

Fig. 1 N_2 adsorption-desorption isotherms of activated carbons obtained from SM samples

The examination of porous texture parameters determined by N_2 sorption at -196℃ (Table 5) reveals that larger surface area is obtained for c-SMd based ACs. For these ACs surface area ranges from 411 m^2/g to 432 m^2/g, while for c-SMc based ACs surface area ranges only from 236 m^2/g to 267 m^2/g. The higher surface area for AC-SMd samples can be explained by the higher microporosity achieved for these ACs (~77-82% of the total pore volume). It can be seen as well that in general an increase of activation time does not cause significant changes in surface area of studied ACs. Nevertheless, maximal surface area development for c-SMc based ACs is already achieved after 30 min activation. In the case of c-SMd based ACs the surface area achieved after 30 min activation (428 m^2/g) is very close to the maximal surface area value (432m^2/g) recorded in the case of AC_{45}-SMd sample. As mentioned by Lima et al. (Lima and Marshall 2005), maximal surface area at lower activation times is desirable because of reduced manufacturing costs of ACs.

3.3 Adsorption study

The Cr speciation forms in solution under various conditions and the role of the carbon surface properties in the removal of these species are a key for clarifying and determining the removal process of Cr(VI) by ACs (Valix *et al.* 2006). In aqueous solution Cr(VI) exists as five main species, i.e., H_2CrO_4, $HCrO_4^-$, CrO_4^{2-}, $HCr_2O_7^-$ and $Cr_2O_7^{2-}$, which distribution depends on pH (Di Natale *et al.* 2007, Demiral *et al.* 2008, Duranoğlu *et al.* 2012, Miretzky and Cirelli, 2010, Parlayici-Karatas and Pehlivan, 2012). In acidic conditions (pH<4) the dominant form is $HCrO_4^-$. Its adsorption by ACs can be explained by the following mechanisms (Di Natale *et al.* 2007, Mohan and Pittman Jr 2006, Liu *et al.* 2007, Miretzky and Cirelli 2010, Duranoğlu *et al.* 2012): i) an electrostatic attraction with protonated acidic groups or protonated basic surface sites; ii) AC oxidation by $HCrO_4^-$ mechanism in which Cr(VI) is reduced to Cr(III) and thus eventually adsorbed on AC external surface. Nowadays a combination of both, or so called a “coupled adsorption-reduction” mechanism, described by Park et al. (Park *et al.* 2008), is widely accepted as the true mechanism of Cr(VI) adsorption by biomaterials under acidic conditions. It comprises: i) direct reduction of Cr(VI) to Cr(III) in the aqueous solution by electro-donor groups of the adsorbent, and Cr(III) complexation on the adsorbent surface or Cr(III) remaining in the aqueous

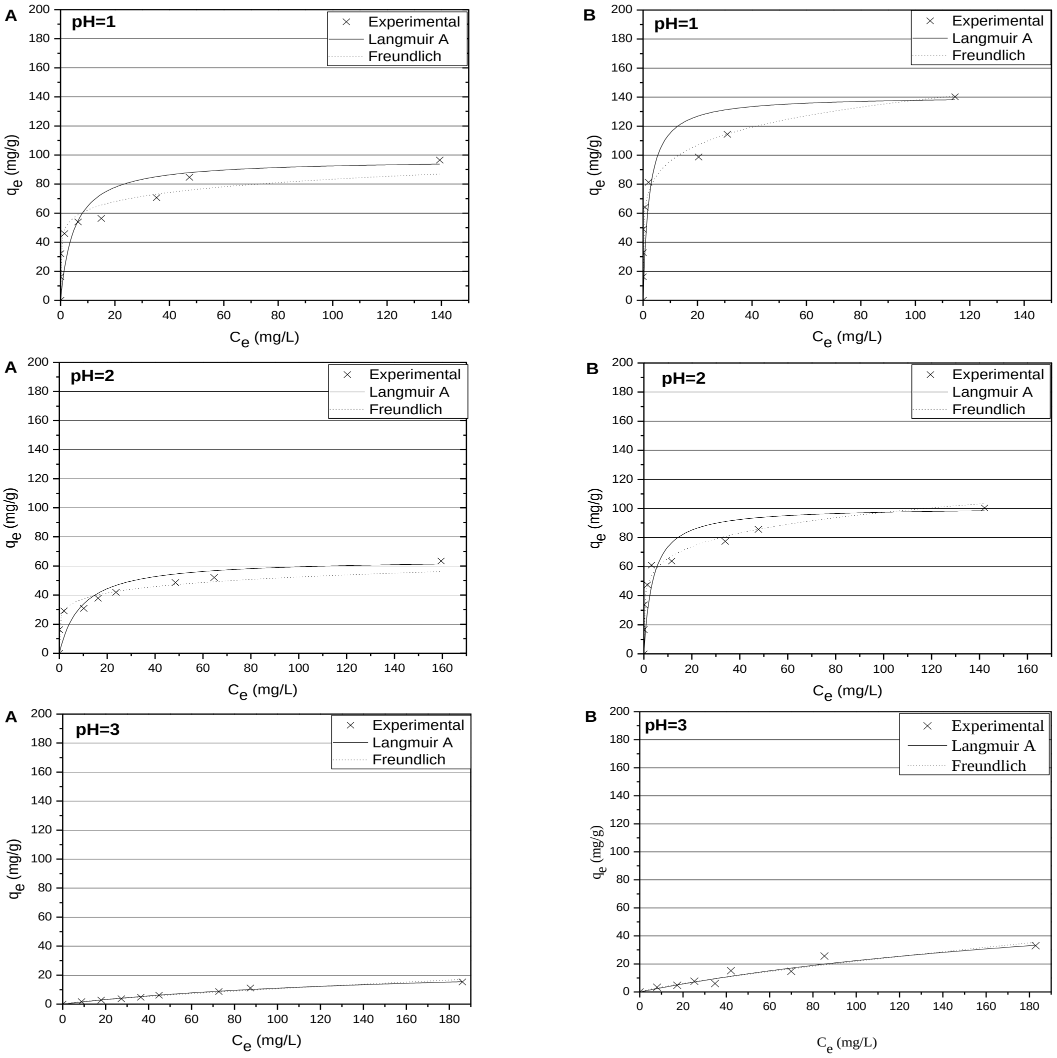

Fig. 2 Experimental and theoretical isotherms of Cr (VI) at different pH for AC_{30}-SMc sample (A) and AC_{30}-SMd sample (B)

phase; or ii) indirect reduction mechanism including the binding of anionic Cr(VI) to the positively-charged groups present on the bio-material surface and further reduction of Cr(VI) to Cr(III) by adjacent electron-donor groups, and then complexation on the surface or release into the aqueous phase of the reduced Cr(III). Which one of those mechanisms, i.e., direct or indirect, is the leading/dominant one is not clear since both are depending on pH, temperature, type of biomaterial and metal concentration. Nevertheless, the authors have shown irrefutable proof that removal of Cr(VI) is mainly due to reduction of Cr(VI) to Cr(III). Similar observation has been reported for ACs as well. Duranoğlu *et al*. (2012) found that 78% of adsorbed Cr is in its trivalent from. Obviously, the removal of Cr(VI) is mainly due to reduction of Cr(VI) to Cr(III). However the presence of Cr(VI) on ACs surface is somehow a proof that removal of Cr(VI) occurs through an indirect reduction mechanism.

3.3.1 Influence of solution pH

The crucial factor affecting adsorption of ionic species from solution is pH. Solution pH variation changes ACs surface charge as well as the state and stability of different metals speciation forms in the solution. Inasmuch as several investigations have shown that AC adsorption of Cr(VI) is favoured at low pH (Khezami and Capart 2005, Hu *et al.* 2003, Demiral *et al.* 2008, Duranoğlu *et al.* 2012), the effect of pH on the removal of Cr(VI) by manure ACs is tested in the solution pH range from 1.0 to 3.0. It is revealed that maximum Cr(VI) removal occurs at pH 1.0 for both samples and decrease with increasing pH (Figs. 2(A)-(B)).

This behavior can be explained by the surface nature of the adsorbent at different pH and Cr(VI) speciation in the solution. It is known that the dominant form of Cr(VI) at pH between 1.0 and 4.0 is $HCrO_4^-$ (Demiral *et al.* 2008, Khezami and Capart 2005, Duranoğlu *et al.* 2012). So that anion form should be preferentially adsorbed by the ACs via positively charged carbon surface. On the other hand, at pH 1.0, in accordance with pH_{pzc} values of AC_{30}-SMc and AC_{30}-SMd samples, i.e., 10.9 and 11.3, respectively, the AC functional groups are highly protonated and AC surface is loaded with positive charges. Inasmuch as studied ACs are characterized by low content of oxygen and relatively high content of nitrogen, a positive charge is expected to be due to protonation of nitrogen containing groups or π-electron system of the basal planes of AC (Boehm 1994). Thus, a strong electrostatic attraction between positively charged AC_{30}-SMc and AC_{30}-SMd surfaces and $HCrO_4^-$ ions becomes possible. The decrease in Cr(VI) removal with increasing pH coincides with decreased concentration of the positive charges present on the surface of activated carbon.

As already mentioned, Cr(VI) removal by ACs can be explained not only by its adsorption on AC surface but also by its reduction to the less toxic Cr(III) form. Cr(III) can be further adsorbed on AC or released in the solution. The reduction of Cr(VI) to Cr(III) preferentially occurs at acidic condition as described in (Di Natale *et al.* 2007, Duranoğlu *et al.* 2012, Parlayici-Karatas and Pehlivan 2012) by the following reaction

$$4HCrO_4^- + 3C + 16H^+ \rightarrow 4Cr^{3+} + 10H_2O + 3CO_2$$

In order to check if such a mechanism is involved in the removal of Cr(VI) by studied ACs, the chromium distribution during Cr(VI) adsorption experiments on AC_{30}-SMc and AC_{30}-SMd at different pH is assessed and shown in Fig. 3. It is clear that beside adsorption, reduction of Cr(VI) to Cr(III) also occurs. The highest amount of Cr(VI) for both samples under consideration, i.e., AC_{30}-SMc and AC_{30}-SMd, is removed (i.e., adsorbed and reduced) at the lowest pH, but at such pH significant part of the removed Cr(VI) remains in the solution in its reduced Cr(III) form. Clearly Cr(VI) reduction to Cr(III) is superior at pH 1.0 and the amount of Cr(III) remaining into the solution significantly decreases with pH increase. This is due to the following possibilities which probably may occur simultaneously but cannot be distinguished at the current stage of research: i) with pH increase less $HCrO_4^-$ ions are bonded on AC surface, respectively less $HCrO_4^-$ ions can be reduced to Cr(III) by adjacent electron-donor group/dissolved organic carbon; and ii) Cr(III) cations are preferentially involved in complexation reactions with AC surface groups. With pH increase positively charged Cr(III) ions, if formed, are more adsorbed on AC as it becomes more negatively charged and thus the amount of free Cr(III) in the solution at equilibrium is decreased. At pH 2 lower amount of Cr(VI) is removed (adsorbed and reduced) compared to those at pH 1 but higher amount of Cr_{tot} is adsorbed. Similar peculiarity is observed in an earlier study (Gonsalvesh *et al.* 2016b), which is considered as a more desirable result as Cr(III) is less toxic but in the environment an oxidation of Cr(III) to Cr(VI) can occur. Removal/adsorption at pH 3 is not favorable at all since 80-90% of Cr remains in the solution at equilibrium. At all studied pH values

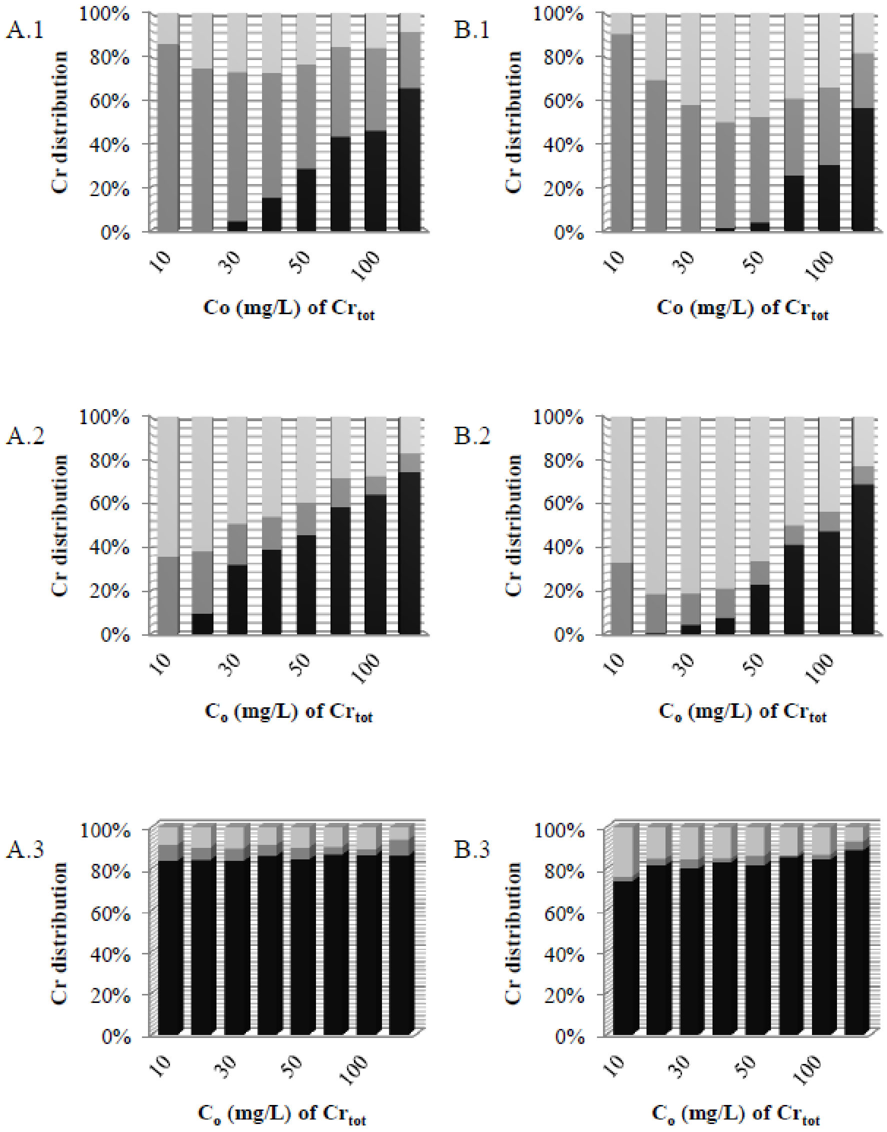

Fig. 3 Chromium distribution during Cr(VI) adsorption experiments on AC$_{30}$-SMc (A) and AC$_{30}$-SMd (B) samples at different pH: (1) pH=1; (2) pH=2; (3) pH=3. Different colors of the columns represent adsorbed Cr$_{tot}$ (light grey), C$_e$ of Cr(III) in the solution (dark grey) and C$_e$ of Cr(VI) in the solution (black)

AC$_{30}$-SMd sample performs better in Cr(VI)/Cr$_{tot}$ removal/adsorption compared to AC$_{30}$-SMc sample.

3.3.2 Influence of activation time

The influence of the activation time on Cr(VI) adsorption properties of studied ACs is also investigated. Adsorption experiments are performed at pH 2 since highest Cr$_{tot}$ adsorption by AC$_{30}$-SMc and AC$_{30}$-SMd samples occurs at that pH. The obtained results are visualized in Fig. 4(A) for all SMc AC samples and in Fig. 4(B) for all SMd AC samples.

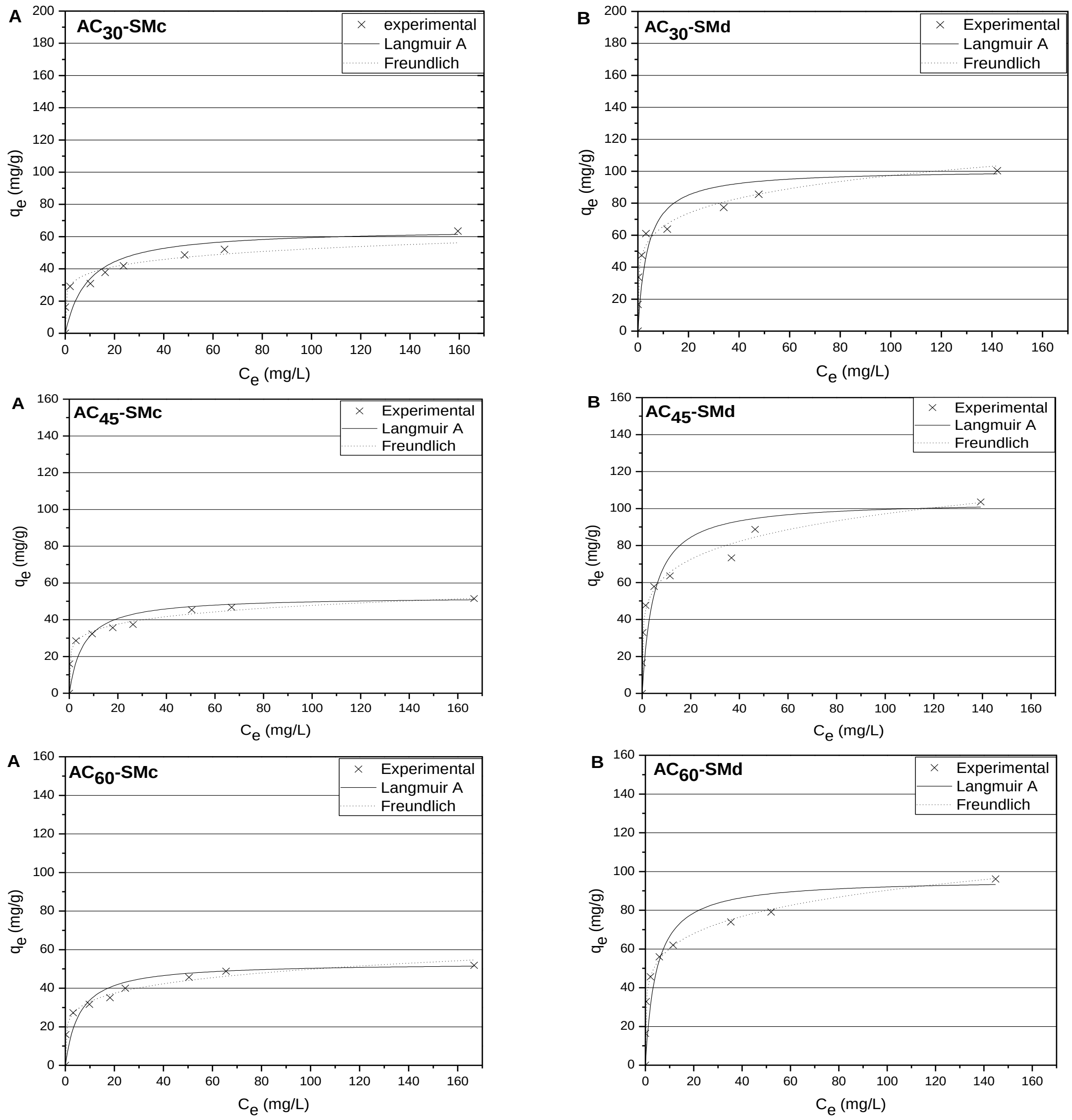

Fig. 4 Experimental and theoretical isotherms of Cr (VI) at pH=2: (A) for AC_{30}-Mc, AC_{45}-SMc and AC_{60}-SMc samples; (B) for AC_{30}-SMd, AC_{45}-SMd and AC_{60}-SMd samples

It can be seen that Cr(VI) isotherms of ACs prepared from c-SMc char (Fig. 4(A)) are similar. With increasing activation time Cr(VI) removal somewhat decreases. For AC_{30}-SMd, AC_{45}-SMd and AC_{60}-SMd samples considerable difference in Cr(VI) removal with increasing activation time cannot be observed as well (Fig. 4(B)). It is essential to stress that ACs prepared from c-SMd show higher Cr(VI) removal than ACs prepared from c-SMc. Confirmation is also found in the calculated Langmuir adsorption isotherm parameter, i.e., maximum adsorption capacity (Table 6).

The higher Cr(VI) removal capacity for all SMd AC samples corresponds to their better developed porous texture and surface area (see Table 5), and to their slightly higher basic character.

Table 6 Langmuir and Freundlich parameters and correlation coefficients of Cr(VI) adsorption isotherms

Sample	pH	Langmuir-A				Freundlich		
		K_L L/mg	q_m mg/g	R^2	R_L	K_F (mg/g (L/mg)$^{1/n}$	n	R^2
AC_{30}-SMc	1	0.20	97.09	0.9883	0.025	46.46	7.88	0.9449
	2	0.11	64.94	0.9860	0.045	26.66	6.81	0.9472
	3	0.01	29.33	0.9099	0.460	0.33	1.33	0.9877
AC_{45}-SMc	2	0.17	52.63	0.9957	0.029	24.00	6.68	0.9902
AC_{60}-SMc	2	0.17	53.19	0.9970	0.028	21.83	5.58	0.9886
AC_{30}-SMd	1	0.45	140.85	0.9923	0.011	66.59	6.33	0.8317
	2	0.27	101.01	0.9930	0.018	44.03	5.81	0.9862
	3	0.00	81.30	0.3049	0.564	0.56	1.25	0.9057
AC_{45}-SMd	2	0.21	104.17	0.9877	0.022	42.08	5.50	0.9919
AC_{60}-SMd	2	0.22	96.15	0.9915	0.022	40.04	5.66	0.9965

3.3.3 Adsorption isotherms study

The results from Langmuir and Freundlich models application on the data of Cr(VI) adsorption by prepared manure based ACs are presented in Table 6. The Langmuir-A equation for all of the applied adsorption processes gives a better fit except for those performed at pH 3. The linearizations according to Langmuir-B equation produce a much lower correlation coefficient and were therefore not included in the table. The Langmuir model describes better current Cr(VI) adsorption data in most of studied circumstances and therefore a monolayer coverage chemisorption of the Cr(VI) on the surface of the ACs can be assumed. Exception is observed for adsorption processes performed at pH 3 where correlation coefficients of Freundlich model are clearly higher, meaning that the adsorption mechanism changes. It is already mentioned that not only Cr(VI) is involved in the adsorption process, but that also Cr(III) is adsorbed. A competitive/synergetic process does influence this adsorption mechanism, resulting in a change of dominating adsorption isotherm as a function of pH and thus a change in adsorption characteristics.

Calculated Langmuir monolayer adsorption capacities q_m (Table 6) confirm aforementioned peculiarities related to the influence of pH, activation time and surface area. It is observed that: i) q_m is maximal at pH 1 and decrease with increasing pH for both types of ACs prepared from c-SMc and c-SMd; ii) q_m is not significantly altered with increasing activation time for the studied ACs since for each series of ACs the differences in textural parameters are relatively small; iii) higher q_m values are calculated for ACs characterized with higher surface area and prepared from c-SMd. The obtained q_m values are comparable to other studies reported in the literature on Cr(VI) removal by ACs and raw and modified lignocellulosic materials ((Miretzky and Cirelli 2010, Duranoğlu *et al*. 2012) and ref. therein). It can even be stated that ACs produced in our study, especially those from c-SMd, have greater Cr(VI) adsorption capacity compared to reported ones. The favorability of Cr(VI) adsorption process can be obtained from the magnitude of R_L value which indicates the type of Langmuir isotherm: irreversible (R_L=0), favorable (0<R_L<1), linear (R_L=1) and unfavorable (R_L>1). The calculated values of R_L shown in Table 6 indicate that Cr(VI) adsorption on ACs prepared from swine manure is favorable in all cases.

4. Conclusions

Our study demonstrates that swine manures, i.e., de-watered SM cake (SMc) and solid digestate (SMd), are suitable precursors for production of low cost ACs through pyrolysis and subsequent physical activation by steam. The effectiveness of the prepared ACs towards Cr(VI) removal in aqueous solutions is evaluated and it is revealed that prepared ACs demonstrate great Cr (VI) removal capacity occurring through a “coupled adsorption-reduction” mechanism. The removal of Cr(VI) is found to be pH dependent and superior at pH 1. However at that pH value significant part of the removed Cr(VI) remain in the solution in its reduced form, i.e., Cr(III). Lower amount of Cr(VI) is removed at pH 2 compared to those at pH 1 but higher amount of Cr_{tot} is adsorbed. It is therefore advisable to remove both Cr(VI) and Cr(III) by the same ACs at the appropriate pH 2. For the studied ACs the removal capacity towards Cr(VI) is not significantly altered and is almost independent of the activation time. This is a desirable result as a shorter activation time reduces the manufactory cost. Higher Cr(VI) removal capacity is demonstrated by ACs prepared from SMd sample having better porous texture.

Acknowledgments

The authors are grateful to Greet Cuyvers and Elsy Thijssen for performing ICP analyses.

References

Azuara, M., Kersten, S.R.A. and Kootstra, A.M.J. (2013), “Recycling phosphorus by fast pyrolysis of pig manure: Concentration and extraction of phosphorus combined with formation of value-added pyrolysis products”, *Biom. Bioenergy*, **49**, 171-180.

Bandosz, T.J. (2006), *Activated Carbon Surfaces in Environmental Remediation*, Elsevier.

Barkat, M., Nibou, D., Chegrouche, S. and Mellah, A. (2009), “Kinetics and thermodynamics studies of chromium(VI) ions adsorption onto activated carbon from aqueous solutions”, *Chem. Eng. Proc.: Proc. Intensific.*, **48**(1), 38-47.

Boehm, H.P. (1994), “Some aspects of the surface chemistry of carbon blacks and other carbons”, *Carbon*, **32**(5), 759-769.

Brunauer, S., Emmett, P.H. and Teller, E. (1938), “Adsorption of gases in multimolecular layers”, *J. Am. Chem. Soc.*, **60**, 309-319.

Cantrell, K.B., Hunt, P.G., Uchimiya, M., Novak, J.M. and Ro, K.S. (2012), “Impact of pyrolysis temperature and manure source on physicochemical characteristics of biochar”, *Biores. Technol.*, **107**, 419-428.

Channiwala, S.A. and Parikh, P.P. (2002), “A unified correlation for estimating HHV of solid, liquid and gaseous fuels”, *Fuel*, **81**(8), 1051-1063.

Demiral, H., Demiral, İ., Tümsek, F. and Karabacakoğlu, B. (2008), “Adsorption of chromium(VI) from aqueous solution by activated carbon derived from olive bagasse and applicability of different adsorption models”, *Chem. Eng. J.*, **144**(2), 188-196.

Di Natale, F., Lancia, A., Molino, A. and Musmarra, D. (2007), “Removal of chromium ions form aqueous solutions by adsorption on activated carbon and char”, *J. Hazard. Mater.*, **145**(3), 381-390.

Duranoğlu, D., Trochimczuk, A.W. and Beker, U. (2012), "Kinetics and thermodynamics of hexavalent chromium adsorption onto activated carbon derived from acrylonitrile-divinylbenzene copolymer", *Chem. Eng. J.*, **187**, 193-202.

European Environment Agency (2009), *Part B: Sectoral Guidance Chapters, 4b*. Manure management, EMEP/EE Air Pollutant Emission Inventory Guidebook.

Foo, K.Y. and Hameed, B.H. (2010), "Insights into the modeling of adsorption isotherm systems", *Chem. Eng. J.*, **156**(1), 2-10.

Gonsalvesh, L., Marinov, S.P., Gryglewicz, G., Carleer, R. and Yperman, J. (2016a), "Preparation, characterization and application of polystyrene based activated carbons for Ni(II) removal from aqueous solution", *Fuel Proc. Technol.*, **149**, 75-85.

Gonsalvesh, L., Yperman, J., Carleer, R., Mench, M., Herzig, R. and Vangronsveld, J. (2016b), "Valorisation of heavy metals enriched tobacco biomass through slow pyrolysis and steam activation", *J. Chem. Technol. Biotechnol.*, **91**(6), 1585-1595.

Ho, Y.S. (2006), "Isotherms for the sorption of lead onto peat: Comparison of linear and non-linear methods", *Pol. J. Environ. Stud.*, **15**(1), 81-86.

Hu, Z., Lei, L., Li, Y. and Ni, Y. (2003), "Chromium adsorption on high-performance activated carbons from aqueous solution", *Separat. Purificat. Technol.*, **31**(1), 13-18.

Khezami, L. and Capart, R. (2005), "Removal of chromium(VI) from aqueous solution by activated carbons: Kinetic and equilibrium studies", *J. Hazard. Mater.*, **123**(1-3), 223-231.

Kinniburgh (1986), "General purpose adsorption isotherms", *Environ. Sci. Technol.*, **20**, 895-904.

Lima, I.M. and Marshall, W.E. (2005), "Granular activated carbons from broiler manure: Physical, chemical and adsorptive properties", *Biores. Technol.*, **96**(6), 699-706.

Liu, S.X., Chen, X., Chen, X.Y., Liu, Z.F. and Wang, H.L. (2007), "Activated carbon with excellent chromium(VI) adsorption performance prepared by acid-base surface modification", *J. Hazard. Mater.*, **141**(1), 315-319.

McKendry, P. (2002a), "Energy production from biomass (part 1): Overview of biomass", *Biores. Technol.*, **83**(1), 37-46.

McKendry, P. (2002b), "Energy production from biomass (part 2): Conversion technologies", *Biores. Technol.*, **83**(1), 47-54.

Miretzky, P. and Cirelli, A.F. (2010), "Cr(VI) and Cr(III) removal from aqueous solution by raw and modified lignocellulosic materials: A review", *J. Hazard. Mater.*, **180**(1-3), 1-19.

Mohan, D. and Pittman Jr, C.U. (2006), "Activated carbons and low cost adsorbents for remediation of tri- and hexavalent chromium from water", *J. Hazard. Mater.*, **137**(2), 762-811.

Park, D., Lim, S.R., Yun, Y.S. and Park, J.M. (2008), "Development of a new Cr(VI)-biosorbent from agricultural biowaste", *Biores. Technol.*, **99**(18), 8810-8818.

Parlayici-Karatas, S. and Pehlivan, E. (2012), "Removal of hexavalent chromium using modified pistachio shell", *Adv. Environ. Res.*, **1**(2), 167-179.

Ro, K.S., Cantrell, K.B. and Hunt, P.G. (2010), "High-temperature pyrolysis of blended animal manures for producing renewable energy and value-added biochar", *Ind. Eng. Chem. Res.*, **49**, 10125-10131.

Schnitzer, M.I., Monreal, C.M. and Jandl, G. (2008), "The conversion of chicken manure to bio-oil by fast pyrolysis. III. Analyses of chicken manure, bio-oils and char by Py-FIMS and Py-FDMS", *J. Environ. Sci. Health B*, **43**(1), 81-95.

Smets, K., Adriaensens, P., Reggers, G., Schreurs, S., Carleer, R. and Yperman, J. (2011), "Flash pyrolysis of rapeseed cake: Influence of temperature on the yield and the characteristics of the pyrolysis liquid", *J. Analyt. Appl. Pyrolys.*, **90**(2), 118-125.

Stals, M., Carleer, R., Reggers, G., Schreurs, S. and Yperman, J. (2010), "Flash pyrolysis of heavy metal contaminated hardwoods from phytoremediation: Characterisation of biomass, pyrolysis oil and char/ash fraction", *J. Analyt. Appl. Pyrolys.*, **89**(1), 22-29.

Stoeckli, F., Daguerre, E. and Guillot, A. (1999), "The development of micropore volumes and widths during physical activation of various precursors", *Carbon*, **37**, 2075-2077.

Tsai, W.T., Liu, S.C., Chen, H.R., Chang, Y.M. and Tsai, Y.L. (2012), "Textural and chemical properties of swine-manure-derived biochar pertinent to its potential use as a soil amendment", *Chemosph*., **89**(2), 198-203.

Uchimiya, M., Bannon, D.I., Wartelle, L.H., Lima, I.M. and Klasson, K.T. (2012), "Lead retention by broiler litter biochars in small arms range soil: Impact of pyrolysis temperature", *J. Agricult. Food Chem*., **60**(20), 5035-5044.

Valix, M., Cheung, W.H. and Zhang, K. (2006), "Role of heteroatoms in activated carbon for removal of hexavalent chromium from wastewaters", *J. Hazard. Mater*., **135**(1-3), 395-405.

Xiu, S., Shahbazi, A., Shirley, V. and Cheng, D. (2010), "Hydrothermal pyrolysis of swine manure to bio-oil: Effects of operating parameters on products yield and characterization of bio-oil", *J. Analyt. Appl. Pyrolys*., **88**(1), 73-79.

WL